Electromagnetic transitions and structure in the $Z = N$ nucleus ^{46}V

F. Brandolini,[1] N. H. Medina,[2] R. V. Ribas,[2] S. M. Lenzi,[1] A. Gadea,[3] C. A. Ur,[1,4] D. Bazzacco,[1] R. Menegazzo,[1]
P. Pavan,[1] C. Rossi-Alvarez,[1] A. Algora-Pineda,[3] G. de Angelis,[3] M. De Poli,[3] E. Farnea,[3] N. Mărginean,[3,4] T. Martinez,[3]
D. R. Napoli,[3] M. Ionescu-Bujor,[4] A. Iordachescu,[4] J. A. Cameron,[5] S. Kasemann,[6] I. Schneider,[6] J. M. Espino,[7]
and J. Sanchez-Solano[8]

[1]*Dipartimento di Fisica and INFN, Padova, Italy*
[2]*Instituto de Física, Universidade de São Paulo, São Paulo, Brazil*
[3]*INFN, Laboratori Nazionali di Legnaro, Legnaro, Italy*
[4]*National Institute for Physics and Nuclear Engineering, Bucharest, Romania*
[5]*McMaster University, Ontario, Canada*
[6]*Institut für Kernphysik der Universität zu Köln, Köln, Germany*
[7]*Departamento de Fisica, Universidad de Sevilla, Sevilla, Spain*
[8]*Departamento de Física Teorica, Universidad Autónoma, Cantoblanco, Madrid, Spain*

The nucleus ^{46}V has been studied in the reaction ^{24}Mg$(^{28}$Si$, \alpha pn)^{46}$V at 115 MeV beam energy, using both Au and Pb backed targets. Lifetimes were obtained for 14 levels with DSAM analysis. Experimental $B(E2)$ reduced transition probabilities are well reproduced by the large scale shell model. The observed levels could be organized in bands with a rather good K value.

I. INTRODUCTION

In recent years an extensive experimental study of the structure of nuclei in the middle of the $1f_{7/2}$ shell has been made at LNL, in particular for ^{48}Cr, ^{49}Cr, ^{50}Cr, and ^{47}V [1–4]. Rotorlike bands have been found. Since experimental B(E2) values of good quality are essential to substantiate the rotational collectivity, the lifetimes of many levels [2–4] have been determined with careful doppler shift attenuation method (DSAM) analysis. Large scale shell model (LSSM) calculations in the full fp configuration space [5] reproduce very well the excitation energies of the observed natural parity levels and transition probabilities, while the unnatural parity bands are reasonably reproduced by extending the configuration space to include a $d_{3/2}$ hole [6].

In this context new results are presented here for the $Z = N$ nucleus ^{46}V, which has recently aroused great interest owing to its special peculiarities [7–11]. As shown in the level scheme of Fig. 1, coexistence of natural parity $T = 1$ states with $T = 0$ and unnatural parity states occurs at low excitation energy, so isospin selection rules and isospin mixing can be tested. This nucleus has previously been studied at the spectrometer GASP of LNL with the reaction ^{24}Mg on ^{28}Si at 100 MeV bombarding energy, using a thin self-supporting target [7]. A detailed level scheme was obtained and compared with LSSM predictions. Two other experimental works in ^{46}V also appeared recently: a less extensive level scheme was obtained using the PEX array [9] in the same reaction as in Ref. [7], but at a bombarding energy of 87 MeV. Low-lying levels have been studied in detail using the reaction ^{46}Ti$(p,n)^{46}$V at 15 MeV [10]. Preliminary data of a plunger lifetime measurement in the reaction ^{32}S$(^{16}$O$,pn)^{46}$V have been reported [11]. Finally, the $T = 1$ band has been extended up to $I = 10^+$ at Gammasphere/FMA [12].

The present work, performed at LNL, complements the previous one [7] and has the main aim to extend the study of the electromagnetic properties in order to understand better the structure of this nucleus. No lifetime values in the DSAM range have so far been reported.

II. EXPERIMENTAL PROCEDURE AND RESULTS

The nucleus ^{46}V was populated in the reaction ^{28}Si on ^{24}Mg at 115 MeV bombarding energy, using 0.8mg/cm^2 targets of ^{24}Mg backed with 15mg/cm^2 either of Au or of Pb. The incident energy in the center-of-mass reference was the same as in the previous experiment, so that experimental intensities can be directly compared. Gamma rays were detected with the GASP array, comprising 40 Compton-suppressed HPGe detectors and an 80-element BGO ball which acts as a gamma-ray multiplicity filter.

The level scheme of ^{46}V of Fig. 1 is organized in rotational bands of definite K values, as suggested by the appearance of rotational bands in this nuclear region. At high spin it is a simplified version of that of Ref. [7], since mainly levels observed in the present work are shown. However, by virtue of the better energy resolution for Doppler unbroadened peaks, several new transitions have been observed. The levels 6^+ at 3365 keV and 7^+ at 3642 keV, which were not observed in the present experiment, are reported for completeness. The arrow widths are proportional to the line intensities. It may be objected that a K classification for the positive parity levels is not justified, owing to the band irregularity, but the following discussion of the γ transitions will show that it may be appropriate as a first approximation. A summary of experimental data, which includes those of Ref. [7], is reported in Table I.

According to the Gallagher-Moszkowski (GM) rule [8], the presence of $K = 3^+$ and $K = 0^+$ bands is expected at low energy, corresponding to a parallel and antiparallel coupling of the Nilsson orbitals $[321]3/2^-$ occupied by the odd nucle-
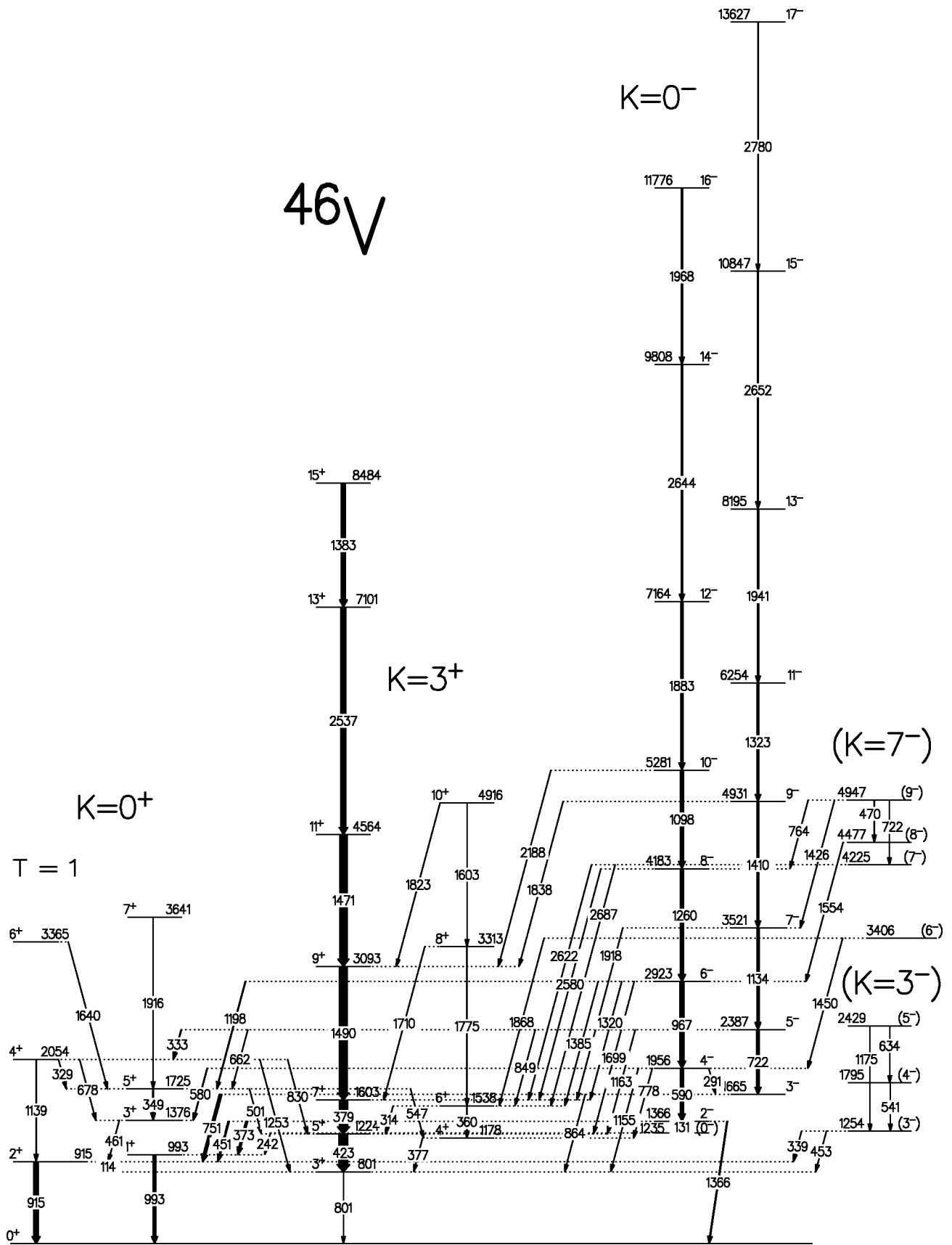
FIG. 1. Level scheme of ^{46}V.

TABLE I. Experimental and theoretical results in ^{46}V. Errors in γ-ray energies are 0.4 keV rising to 1 keV above 2 MeV. Gamma lines in brackets were not observed. Theoretical $B(E2)$ values and branches less than 0.1 are set to 0.

Transition	E_γ exp. keV	E_γ SM keV	$\gamma-$BR exp. %	$\gamma-$BR th. %	τ exp. ps	τ th. ps	$B(E2)$ exp. e^2 fm^4	$B(E2)$ th. e^2 fm^4	$B(M1)$ exp. μ_N^2	$B(M1)$ th. μ_N^2
$K=3^+$										
$5^+\rightarrow3^+$	423.3	496	100	100	903(107) [a]		67(14)	65		
$7^+\rightarrow5^+$	379.3	447	100	100	1080(170) [b]		97(15)	61		
$9^+\rightarrow7^+$	1490.1	1518	100	100	0.70(15) [c]		159(34)	145		
$11^+\rightarrow9^+$	1471.3	1558	100	100	0.85(16) [c]		139(26)	130		
$13^+\rightarrow11^+$	2537.4	2535	100	100	0.10(2) [c]		78(16)	89		
$15^+\rightarrow13^+$	1382.8	1800	100	100	2.7(5)		60(12)	67		
$4^+\rightarrow3^+$	377.9	507	100	100	514(119) [a]		208(50)	296		5×10^{-5}
$6^+\rightarrow4^+$	360.0	294	45(5)	45		783		79		
$6^+\rightarrow5^+$	315.1	306	55(5)	55				187		9×10^{-5}
$8^+\rightarrow6^+$	1775.0	2081	70(8)	78		0.32		113		
$8^+\rightarrow7^+$	1710.0	1939	30(8)	22				36		4×10^{-5}
$10^+\rightarrow8^+$	1603.0	1569	60(9)	64		0.47		96		
$10^+\rightarrow9^+$	1823.0	1988	40(9)	36				31		3×10^{-5}
$K=0^+$										
$2^+\rightarrow0^+$	915.0	993	98.0(4)	95	9.0(23) [a]		138(35)	142		
$2^+\rightarrow3^+$	113.5	128	2.0(4)	5				2.0		0.21
$1^+\rightarrow0^+$	993.2	949	100	100		0.06				1.07
$3_2^+\rightarrow1^+$	(383)	443	<1	0.1		0.54		189		
$3_2^+\rightarrow2^+$	461.4	398	100	99.9	0.29(10) [a]			0.1	2.0(7)	1.07
$3_2^+\rightarrow3^+$	(574)	526	<5	0				1.3		$<10^{-5}$
$4_2^+\rightarrow2^+$	1140.1	1398	8(1)	6		0.13		187		
$4_2^+\rightarrow3^+$	1253.1	1026	14(2)	34				0		0.08
$4_2^+\rightarrow4^+$	(875)	520	<3	1				0.4		0.027
$4_2^+\rightarrow3_2^+$	678.4	499	65(3)	42				0		0.63
$4_2^+\rightarrow5^+$	830.1	530	7(1)	4				0.2		0.032
$4_2^+\rightarrow5_2^+$	328.9	242	6(1)	12				0.2		1.55
$5_2^+\rightarrow3^+$	(923)	784	<10	34		51		7.3		
$5_2^+\rightarrow3_2^+$	349.1	257	74(4)	44				160		
$5_2^+\rightarrow4^+$	547.1	277	8(2)	10				10.2		1×10^{-5}
$5_2^+\rightarrow5^+$	501.4	288	18(2)	13				17		7×10^{-5}
$5_2^+\rightarrow6^+$	(186)	8	<5	0				2.6		7×10^{-5}
$K=0^-$										
$2^-\rightarrow(0^-)$	130.5	44	0.9(2)		1424(600) [a]		160(75)	200		
$4^-\rightarrow2^-$	590.1	684	85.0(9)	99		50		89		
$5^-\rightarrow3^-$	721.6	871	91.2(8)	100		17		183		
$6^-\rightarrow4^-$	967.2	1232	85.3(9)	100	3.3(7) [c,d]		248(55)	203		
$7^-\rightarrow5^-$	1134.0	1360	97.3(9)	100	1.5(3) [c,d]		282(57)	270		
$8^-\rightarrow6^-$	1259.8	1396	94.5(7)	100	0.90(23) [c,d]		271(70)	242		
$9^-\rightarrow7^-$	1410.0	1547	98.8(4)	100	0.61(13) [c,d]		237(52)	234		
$10^-\rightarrow8^-$	1098.4	1350	96.0(6)	100	4.5(9) [c,d]		109(24)	92		
$11^-\rightarrow9^-$	1323.6	1357	100	100	1.1(2) [c]		175(34)	140		
$12^-\rightarrow10^-$	1882.6	2075	100	100	0.23(4)		150(28)	122		
$13-\rightarrow11-$	1940.6	2032	100	100	0.24(5)		124(27)	130		
$14^-\rightarrow12^-$	2644.2	2338	100	100	0.050(15)		126(38)	95		
$15^-\rightarrow13^-$	2651.6	2835	100	100	0.10(2)		62(12)	88		
$16^-\rightarrow14^-$	1969.1	2673	100	100	0.55(15)		50(14)	62		
$17^-\rightarrow15^-$	2780.0	2725	100	100	<0.2		>25	68		

[a]Reference [11].
[b]Reference [20].
[c]Also with a NGTB analysis.
[d]Only from data using lead backing.

ons. The antiparallel coupling gives rise to the $K=0^+$ ground state band, shown on the left of Fig. 1, where the even spin levels have $T=1$. The intense, irregular, positive parity band, based on the yrast 3^+ level and terminating at the 15^+ level, can be approximately described as the $K=3^+$ sequence with favored signature. Some triaxiality has been suggested for positive parity states of this nuclide [9], which may give rise to the large irregularity in signature splitting. A third band, indicated in Fig. 1 with $K=0^-$, is described as due to the excitation a $d_{3/2}$ hole, with equal neutron and proton contributions. The GM rule predicts in this nucleus the presence of $K=0^-$ and $K=3^-$ bands, due to the parallel and antiparallel coupling of the orbitals $[202]3/2^+$ and $[321]3/2^-$. A candidate for the 0^- head of the former band has been observed, but none for the 1^- level. For the the predicted $K=3^-$ band, from the parallel coupling, candidates for its head at 1254 keV, and for the next two levels, have already been observed in Refs. [7,10]. These are weakly populated and not connected to other bands. A band, based on a level at 4225 keV, was already observed in the previous experiment [7] and is now classified as $K=(7^-)$. A $K=7^-$ band is indeed predicted in a Nilsson scheme, as due to the excitation of a nucleon from the $[202]3/2^+$ orbital to the empty $[321]5/2^-$ one, with parallel coupling of the four unpaired nucleons. A $K=8^-$ band has been observed in ^{48}V, which arises in a similar way [19]. The assignment $I=(6^-)$ was made [7] for the level at 3406 keV, which seems to not belong to, or decay to the $K=3^-$ sequence. Finally, several weak $E1$ branches have been observed connecting the $K=0^-$ band to positive parity levels (shown in Table II). In Table I the experimental branches from those levels take into account the observed $E1$ decay.

The present experimental data for the $K=0^+$ band are generally in agreement with those of Ref. [10]. There are two relevant differences: the 383 keV $3_2^+ \to 1^+$ transition, reported there to have an intensity of $1.6(4)\%$, was not found, whereas a 1253 keV $4_2^+ \to 3^+$ transition was observed.

LSSM calculations were performed with the code ANTOINE, using the KB3 residual interactions [5]. Such calculations have already been reported for both positive and negative parity in Ref. [7], where the calculated energies are compared with experimental ones. The only change is that the Kurath term $aT(T+1)$, which regulates the relative position of $T=0$ and $T=1$ levels, has been adjusted as in Ref. [10]. In Table I the calculations for transition energies, $M1$ and $E2$ reduced rates, branching ratios and lifetimes are reported. The branching ratios, in this case, do not account for possible $E1$ branches.

For the lifetime measurements, data were sorted into seven $\gamma - \gamma$ matrices having on the first axis the detectors in rings at $34°$, $60°$, $72°$, $90°$, $108°$, $120°$, $146°$ and on the second axis any of the other 39 detectors. More details about the analysis procedure are reported in Ref. [2]. The program LINESHAPE [13] modified and used in order to allow the narrow gate on transition below (NGTB) procedure [14], which is free from systematic errors related with side-feeding uncertainties. As an example, the NGTB line shape analysis of two transitions in the $K=3^+$ band is shown in Fig. 2. With

TABLE II. $E1$ transitions in ^{46}V. Errors in γ-ray energies are 0.4 keV rising to 1 keV above 2 MeV. γ lines in brackets were not observed.

Transition	E_γ keV	BR %	τ ps	W.u. 10^{-6}	
$0^- \to 1^+$	242.4				
$2^- \to 1^+$	373.0	57(6)	1424(600)^a	5.9	
$2^- \to 2^+$	451.1	21(4)		1.2	$\Delta T=1$
$2^- \to 3^+$	(564)	<0.3			
$3^- \to 2^+$	750.7	91(3)			$\Delta T=1$
$3^- \to 3^+$	864.2	0.8(2)			
$3^- \to 4^+$	(486)	<0.4			
$4^- \to 3^+$	1154.6	1.0(2)	42^b	0.1	
$4^- \to 4^+$	772.2	2.7(5)		1.1	
$4^- \to 5^+$	732.0	0.5(2)		0.2	
$4^- \to 3_2^+$	580.1	9.5(8)		9.0	
$5^- \to 4^+$	(1585)	<0.4(1)	16^b		
$5^- \to 5^+$	1162.8	1.7(4)		0.5	
$5^- \to 6^+$	848.3	1.8(4)		1.4	
$5^- \to 4_2^+$	333.0	5.3(6)		69	$\Delta T=1$
$5^- \to 5_2^+$	662.0	1.4(4)		2.3	
$6^- \to 5^+$	1699.2	2.6(5)	3.3(7)	1.3	
$6^- \to 6^+$	1384.5	3.6(8)		3.5	
$6^- \to 7^+$	1320.0	3.6(7)		4.0	
$6^- \to 5_2^+$	1198.2	4.9(6)		7.4	
$7^- \to 6^+$	(1983)	<0.4	1.5(3)		
$7^- \to 7^+$	1918.0	2.7(6)		2.0	
$7^- \to 6_2^+$	(156)	<0.4			
$8^- \to 7^+$	2579.7	5.5(13)	0.90(23)	2.7	
$8^- \to 8^+$	(870)	<0.5			
$8^- \to 9^+$	(1090)	<0.5			
$9^- \to 8^+$	(1618)	<0.5	0.61(13)		
$9^- \to 9^+$	1837.6	1.2(4)		2.5	
$10^- \to 9^+$	2188.3	4(1)	4.5(9)	0.7	

^{a}Reference [11].
^{b}Calculated rotor values with $\beta=0.27$ were adopted.

an upper coincident transition as a probe, the comparison of its full line shape (upper part of the figure) with the partly suppressed line shape (lower part), obtained with a narrow gate on the lower transition to be studied, provides the lifetime associated to the gating transition. The Northcliffe-Schilling stopping power [15], corrected for atomic shell effects [16], was used. The use of lead as backing material was important in order to extend the lifetime measurement to low members of the $K=0^-$ band. The accuracy of stopping powers is discussed elsewhere [17]. Lifetime values have been obtained for 14 transitions and are reported in Table I. Different analyses were performed. Whenever it was possible the NGTB analysis was used. For completeness, LSSM lifetimes values are reported for levels when no experimental value could be obtained.

Two examples of line shape analysis for transitions in the $K=0^-$ band are displayed in Fig. 3. Lifetimes for 11 levels of the $K=0^-$ band were determined, and led to $B(E2)$ values well reproduced by LSSM calculations, as Fig. 4 shows.
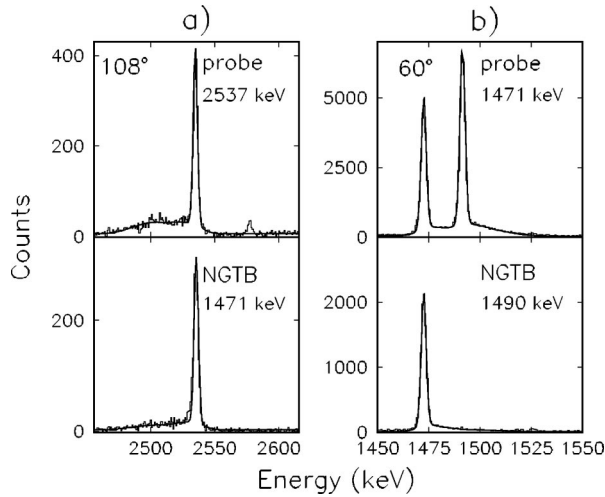
FIG. 2. NGTB lifetime analysis for the 1471 keV $11^+\rightarrow 9^+$ transition (a) and the 1490 keV $9^+\rightarrow 7^+$ transition (b), respectively. A gold backing was employed.

The lifetimes of the 4^- and 5^- levels could not be measured because they are too long, in the range of a plunger measurement. The regular pattern of the low part of the $K=0^-$ band, before the backbending, suggests a rotor-like behavior down to $I=2^-$. The experimental reduced rate for the $2^-\rightarrow(0^-)$ transition, reported in Table I, agrees with this description. The deduced transition quadrupole moment Q_t of approximately $90\,e\,\mathrm{fm}^2$, corresponds to $\beta\simeq 0.27$, which is sligthly smaller than that of the unnatural parity band in ^{47}V [4]. The band turns out to be somewhat more deformed than predicted. The strong back bending of the $\alpha=0$ signature band at $I=10^-$ is accompanied by a sharp decrease of the $B(E2)$ value. Both of them are well reproduced by LSSM, as shown in Table I. The $\Delta I=1$ branches were not observed in the negative-parity band, except for the $4^-\rightarrow 3^-$ transition, which was found with only $1.0(3)\%$ intensity. According to
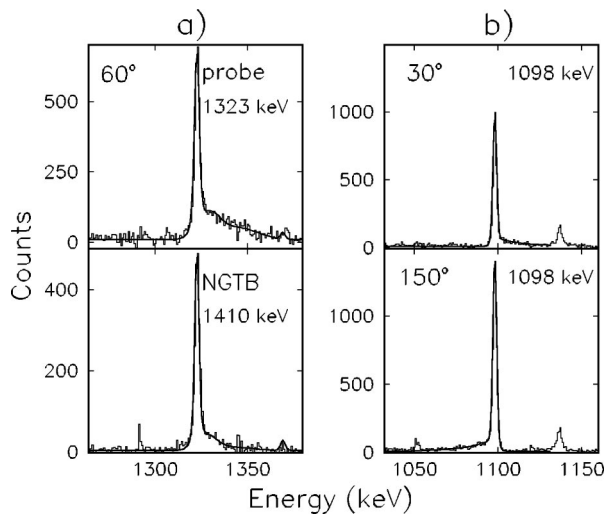

FIG. 3. (a) NGTB lifetime analysis for the 1410 keV $(9^-\rightarrow 7^-)$ transition, using a gold backing (b) Standard line shape analysis for the 1098 keV $(10^-\rightarrow 8^-)$ transition, using a lead backing.
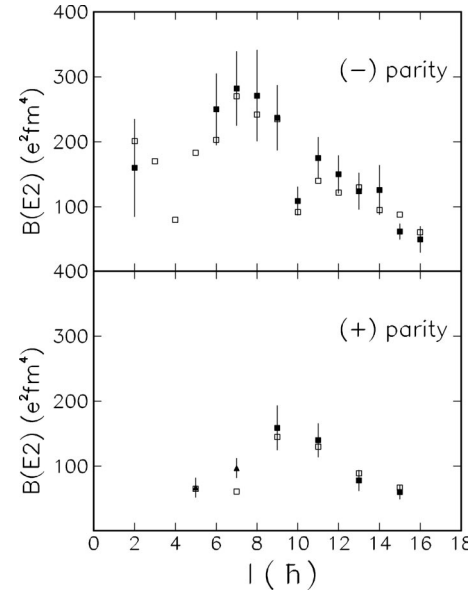

FIG. 4. Experimental $B(E2)$ reduced transition rates in ^{46}V, compared with LSSM predictions (empty squares). Data are taken from the present work (full squares), except for those indicated as full triangles (see text).

the isospin selection rule [18], $\Delta T=0$ $M1$ transitions are predicted to be strongly hindered, so that this branch is likely mainly $E2$.

In the $K=3^+$ band, only the $B(E2)$ values for transitions between levels of the favored signature could be determined and were found to be in good agreement with LSSM calculations, as shown in Fig. 4. A deformation parameter $\beta\simeq 0.22$ is deduced from the reduced rates of $11^+\rightarrow 9^+$ and the $9^+\rightarrow 7^+$ transitions. The agreement between theory and experiment is good also for levels of the $K=0^+$ band. For the $2^+\rightarrow 0^+$ transition in the $T=1$ sequence, we note that the $B(E2)$ value in ^{46}Ti is known to be $191(15)\,e^2\,\mathrm{fm}^4$, while the LSSM prediction is $114\,e^2\,\mathrm{fm}^4$. This is interpreted as arising from mixing of two-hole and four-hole configurations, which bring additional collectivity. This has been also noticed in g-factor measurements [21]. A $B(E2)$ value of $137(35)\,e^2\,\mathrm{fm}^4$ is reported in Ref. [11] for the isobaric analogous transition in ^{46}V, which is much smaller than the experimental value in ^{46}Ti, while it should reasonably be bigger, due to the presence of a valence proton. A more precise lifetime measurement has to be performed for a definitive conclusion. In the case where no lifetimes are available, one can compare calculated and experimental branching ratios. The well-predicted branching ratios for the 4_2^+ level suggest agreeement also for absolute value of reduced rates. It turns out that strong $E2$ transitions only connect levels inside a band, confirming the validity of the K quantum number. This is to some extent surprising, owing to the irregular behavior of positive parity bands.

Detailed data were previously reported for the lower spin levels from the (p,n) reaction [10], where experimental branches are compared with LSSM calculations using both the KB3 and the FPD6 residual interaction. The only significant difference for positive parity levels between those KB3

calculations and the present one, using ANTOINE, is the large value predicted there for the branch of the 501 keV 5_2^+ $\rightarrow 5^+$ transition. The 1.6(4)% branch of the 383 keV 3_2^+ $\rightarrow 1^+$ transition in the $K=0^+$ band, quoted in Ref. [10], is too large to be explained theoretically. In fact, using that branching ratio and the large $B(M1)$ observed [11] for the 461 keV $3_2^+\rightarrow 2^+$ transition, a very large $B(E2)$ value of $55(15)\times 10^2$ e^2 fm^4 would be estimated for the 383 keV transition. One notes that in ^{46}Ti, strongly populated by inelastic scattering in that experiment, the transition $4^-\rightarrow 3^-$ is also 383 keV and is therefore a likely contamination.

Experimental information has also been obtained for the negative parity levels belonging to the $K=(3^-)$ and (7^-) bands, but the agreement with calculations is worse in this case. LSSM calculations predict the 3^-, 4^-, and 5^- levels of a $K=3^-$ band to be close to the corresponding levels of the $K=0^-$ band. Accordingly, the levels based on the 1254 keV level are assigned to a $K=3^-$ band. The negative parity assignment is favored by the fact that no other low-lying positive parity levels are predicted by LSSM. Indeed the spacings, 541 and 634 keV, agree well with the calculated values 571 and 645 keV from LSSM. Although the members of the $K=3^-$ band are calculated to be connected by $E2$ transitions to the $K=0^-$ band, this is not observed. Such interaction between the two bands results in irregularity of the calculated $B(E2)$ values, while the experimental ones seem to be more regular.

In the spectroscopic electric quadrupole moments calculated by LSSM, there is evidence that both the reduction of $B(E2)$ and the backbending at $I=10^-$ are due to a band crossing of the $K=0^-$ band with a $K=7^-$ band. A similar situation occurs for the $K=8^-$ band in ^{48}V [22]. The two high-K bands are interpreted as due to the excitation of a nucleon from the $[202]3/2^+$ orbital to $[321]5/2^-$ with a parallel coupling of the normal parity bands with $K=3^+$ and the $K=4^+$, respectively. It is tempting to relate the (6^-) level at 3406 keV to a 3^- octupole vibration core coupled to a neutron-proton pair with $I=3^+$, the head term of the favored signature sequence. A similar fact seems to occur for the (8^-) level observed at 4257 keV in the cross-conjugate $Z=N$ nucleus ^{50}Mn [22], where the coupling would be with the yrast 5^+ state. In support of this suggestion it is noted that the 3^- level at 3737 keV in ^{40}Ca decays with a collective $B(E3)$ strength of about 27 W.u. Levels with $I=3^-$ of presumable vibrational character are observed in $Z=N$ nuclei ^{44}Ti at 3943 keV, ^{48}Cr at 4067 keV, and ^{52}Fe at 4396 keV. Such 3^- states are also present in $N=Z+2$ nuclei ^{42}Ca at 3446 keV, ^{46}Ti at 3570 keV, and ^{50}Cr at 4052 keV. Unfortunately no $B(E3)$ strengths have so far been determined, so that the suggestion remains unsubstantiated.

The properties of 21 $E1$ transitions, depopulating the levels of the $K=0^-$ band, are summarized in Table II. For eight of them experimental $B(E1)$ values were derived from the present lifetime measurement and for two more levels from lifetimes elsewhere quoted [11]. Furthermore, order of magnitude estimates have been made for the $B(E1)$ rates from the 4^- and 5^- levels, using the rigid rotor estimate with transition quadrupole moment $Q_t=90$ e fm^2. This estimate is favored because the levels seem to be not mixed with those of the $K=3^-$ band.

In a $Z=N$ nucleus $\Delta T=0$, $E1$ transitions are only permitted by the small isospin mixing caused by the Coulomb interaction [18]. The average retardation of $\Delta T=0$, $E1$ transitions with respect to the Weisskopf estimate is about 10^6, as shown in Table II. This is not much larger (perhaps one order of magnitude) than that of non-$Z=N$ nuclei. An explanation has recently been suggested [23]. In any case, this feature is different from what occurs in ^{48}Cr, where the retardation is about 10^9.

Finally one may ask why the 1^- level of the $K=0^-$ band was not observed. No reliable predictions can be made for the lifetime of the 3^- level, which decays mainly $E1$ via the 751 keV$3^-\rightarrow 2^+$ transition. The decay of this level is predicted to have a 366 keV branch to the unobserved 1^- level. Assuming for the $3^-\rightarrow 2^+$ transition a realistic $B(E1)$ value of the order of 10^{-4} W.u., a lifetime of few tens of picoseconds is estimated. In this case a 300–400 keV $E2$ branch to the unobserved 1^- level would be smaller than one percent and could escape the observation.

III. CONCLUSIONS

Much new information has been obtained for the structure of ^{46}V. In spite of the relatively small deformation the classification of the observed levels according to bands of definite K value appears to be successful, at least in first approximation. The agreement with LSSM calculations for positive parity levels is very good. Calculations for negative parity states are satisfactory as they are able to reproduce both the back bending and the drop in the $B(E2)$ value at 10^- in the well-deformed $K=0^-$ band. The possibility of an octupole vibration has been suggested. Several $E1$ transitions have been observed and it has been found that the isospin forbidden $\Delta T=0$ $E1$ transitions are in the average only one order of magnitude retarded with respect to the isospin allowed $\Delta T=1$ $E1$ transitions.

ACKNOWLEDGMENTS

---

[1] S.M. Lenzi *et al.*, Z. Phys. A **354**, 117 (1996).

[2] F. Brandolini *et al.*, Nucl. Phys. **A642**, 387 (1998).

[3] F. Brandolini *et al.*, Phys. Rev. C **60**, 041305(R) (1999).

[4] F. Brandolini *et al*, Nucl. Phys. A (to be published)

[5] E. Caurier *et al.*, Phys. Rev. Lett. **75**, 2466 (1995).

[6] A. Poves and J. Sanchez-Solano, Phys. Rev. C **58**, 179 (1998).

[7] S.M. Lenzi *et al.*, Phys. Rev. C **60**, 021303(R) (1999).

[8] C.G. Gallagher and S.A. Moszkowski, Phys. Rev. **111**, 1282 (1958).

[9] C.D. O'Leary *et al.*, Phys. Lett. B **459**, 73 (1999).

[10] C. Friessner *et al.*, Phys. Rev. C **60**, 011304(R) (1999).

[11] I. Schneider, Ph.D. thesis, Institut für Kernphysik, Köln, 2001; P. v. Brentano *et al.*, Nucl. Phys. **A682**, 48c (2001).

[12] P.E. Garrett *et al.* (unpublished).

[13] J. C. Wells and N. Johnson, Report No. ORNL-6689, 1991 (unpublished).

[14] F. Brandolini and R.V. Ribas, Nucl. Instrum. Methods Phys. Res. A **417**, 150 (1998).

[15] L.C. Northcliffe and R.F. Schilling, Nucl. Data, Sect. A **7**, 233 (1970).

[16] S.H. Sie *et al.*, Nucl. Phys. **A291**, 11 (1977).

[17] F. Brandolini *et al.*, LNL annual report, 1999 (unpublished).

[18] E.K. Warburton and J. Wesener, in *Isospin in Nuclear Physics*, edited by D.H. Wilkinson (North-Holland, Amsterdam, 1969).

[19] R. Ernst *et al.*, Phys. Rev. Lett. **84**, 416 (2000).

[20] A.P. Poletti, E.K. Warburton, and J.W. Olness, Phys. Rev. C **23**, 1550 (1981).

[21] F. Brandolini *et al.*, LNL annual report, 2000 (unpublished).

[22] C.E. Svensson *et al.*, Phys. Rev. C **58**, R2621 (1998).

[23] P.G. Bizzeti (unpublished).